EXPERIMENTAL APPROACH TO UNDERSTAND MINERALOGY AND AQUEOUS ALTERATION HISTORY OF OXIA PLANUM, EXOMARS 2020 LANDING SITE

A.M. Krzesińska[1], B. Bultel[1], J.-C. Viennet[2], D. Loizeau[3] and S.C. Werner[1]

[1]Centre for Earth Evolution and Dynamics, University of Oslo, PO 1028 Blindern, 0316 Oslo, Norway.

[2]Muséum National d'Histoire Naturelle, Institut de Minéralogie, Physique des Matériaux et Cosmochimie, CNRS UMR 7590,

Sorbonne Université, CNRS, F-75005 Paris, France.

[3]Institut d'Astrophysique Spatiale, CNRS/Université Paris-Sud, Université Paris-Saclay, bâtiment 121, 91405 Orsay Cedex, France.

E-mail: a.m.krzesinska@geo.uio.no

www.ptal.eu

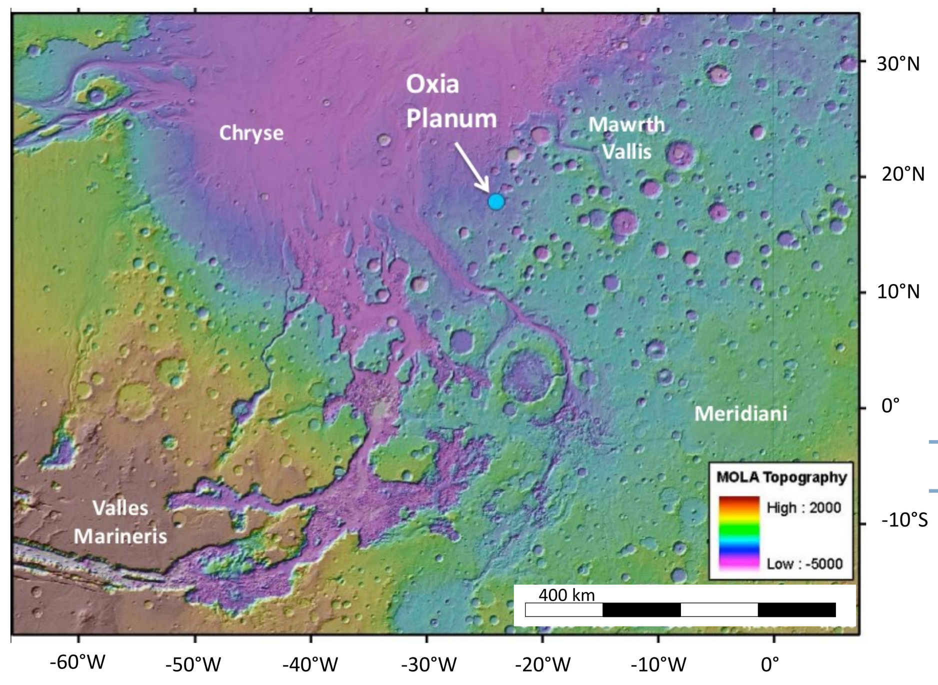

Fig. 1. Oxia Planum location map. Credit: NASA.

EXOMARS 2020/(2022)

- ExoMars is ESA/ROSCOSMOS rover mission to Mars, that will be launched in next years to do in-situ science.
- The final landing site was chosen to be Oxia Planum. Oxia is a wide phyllosilicate-bearing plain located between Mawrth and Ares Valles (Fig. 1).

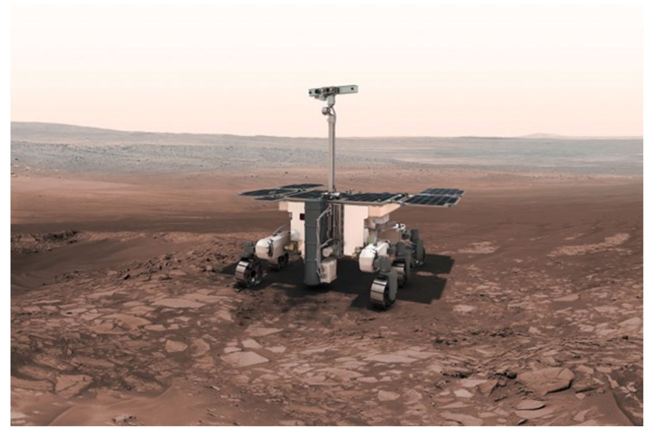

OXIA PLANUM

- Oxia Planum bears record of old and complex history of aqueous alteration.
- Oxia is covered by vast, middle-late Noachian (>3.9 Ga) deposits of Fe,Mg-rich phyllosilicates [1, 2].
- The basement Fe,Mg-phyllosilicates are in places covered by several fluvial morphologies and deltaic deposits, no younger than 3.5 Ga (Fig. 2; [1]). Delta fan deposits consist of Fe^{2+} smectites as well as localized Al-bearing phyllosilicates that formed in an alteration event separate from that which is responsible for formation of basement phyllosilicates [2].
- On top of the stratigraphy, are lava flows related to effusive, Amazonian-aged (~2.6 Ga) volcanism [1, 2].

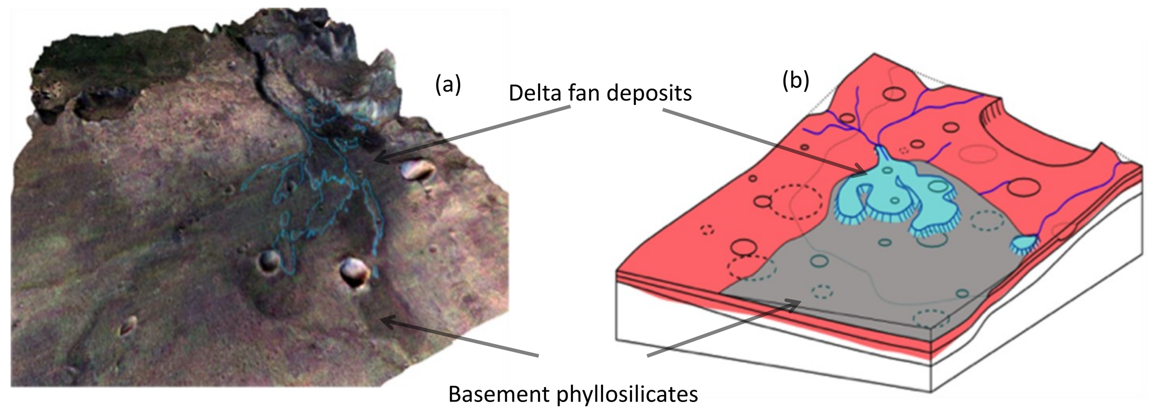

Fig. 2. 3D view of HRSC image (a) and interpretive diagram of the region at the end of Noachian – early Hesperian i.e. delta formation (b). Credit: http://www.insu.cnrs.fr.

We have been performing set of laboratory alteration experiments in controlled, martian conditions, that by analogy with terrestrial environments may be capable to produce best spectral match of vermiculite-like clays detected in Oxia Planum.

BASEMENT PHYLLOSILICATES IN OXIA

- OMEGA and CRISM data reveal that the basement phyllosilicates exhibit large uniformity in terms of spectral features, seldom observed elsewhere [2,3]. The unit is one of the largest phyllosilicate exposures on Mars, with a thickness of more than 10 m. This suggests a single, uniform process of formation or transformation of the phyllosilicate unit.
- The diagnostic absorptions at ~1.4, ~1.9, 2.38 µm and positive slope in 1.1—1.8 region (Fig. 3) indicate that the basement unit consists predominantly of trioctahedral Fe,Mg-rich phyllosilicates [1, 2, 4]. Dioctahedral, Al-rich clays occur only locally.
- The spectral features are consistent with smectite clays (Fe,Mg-rich saponite) or smectite/mica (e.g. vermiculite) [2, 4]. Vermiculite clays are suggested to be the best spectral match (Fig. 1; [2]).
- The mechanism by which vast deposits of trioctahedral (Fe,Mg-vermiculite) phyllosilicates may have formed on Mars is, however, not entirely clear. Likely geological environments that may have led to formation of basement phyllosilicates are: surface weathering (including glacial alteration), hydrothermal conditions, metamorphism or diagenesis [2].

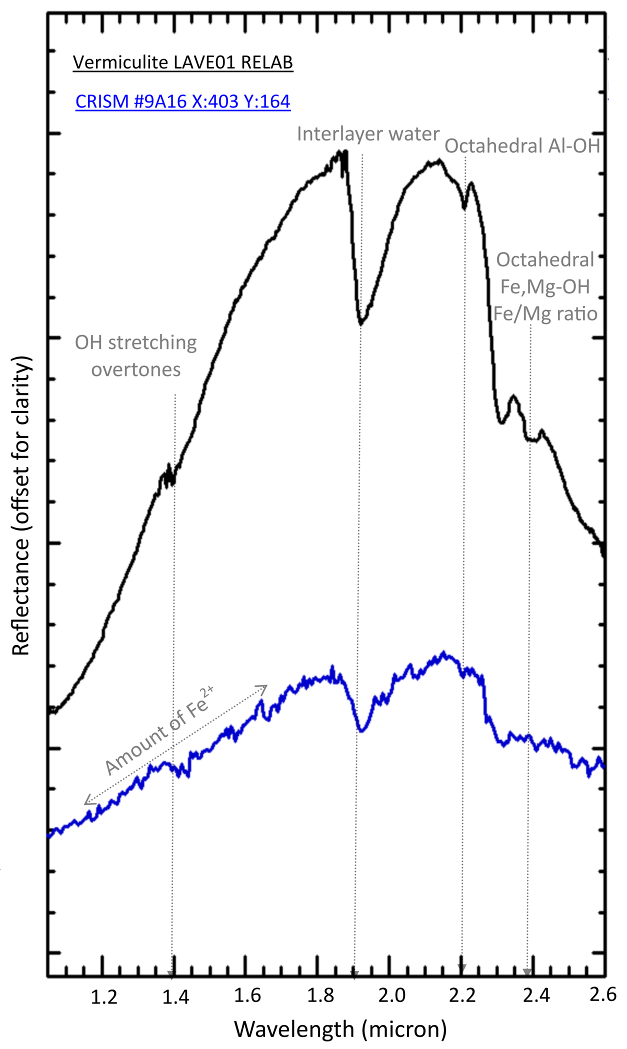

Fig. 3. Spectrum of Fe,Mg-phyllosilicates detected in Oxia Planum by CRISM and comparison with library spectrum of vermiculite.

Characteristic vibrations are indicated.

VERMICULITE FORMATION PATHWAYS

- On the Earth, trioctahedral vermiculite mainly forms in surface weathering environments [5-8], although hydrothermal environments are also discussed [6, 9].
- It is predominantly product of alteration of mica, specifically biotite [5, 6], in which interlayer K cations are replaced by Mg or Fe and H_2O molecules (Fig. 4a-b).
- Assuming presence of biotite-bearing crystalline rocks in the Oxia Planum basement (e.g. trachytes or trachyandesites, such as reported in Gale Crater by [10]), vermiculitization of biotite could be a potential mechanism to form the observed phyllosilicates.
- Alternatively, vermiculite may form by alteration of chlorite by dissolution-precipitation [5, 7] or by chemical oxidation [8]. However, the latter mechanism produces mostly dioctaheral vermiculite (Fig. 4c).
- The presence of chlorite deposits in places on Mars [3] and the highly oxidative nature of martian soil since Hesperian, suggest that alteration of chlorite by e.g. peroxide-rich fluids, in 'deltaic' conditions in Oxia could have been another likely mechanism to form vermiculite.
- However, in order to assess the relevance of such mechanisms to operate on Noachian Mars, influence of atmospheric CO_2 has to be tested.

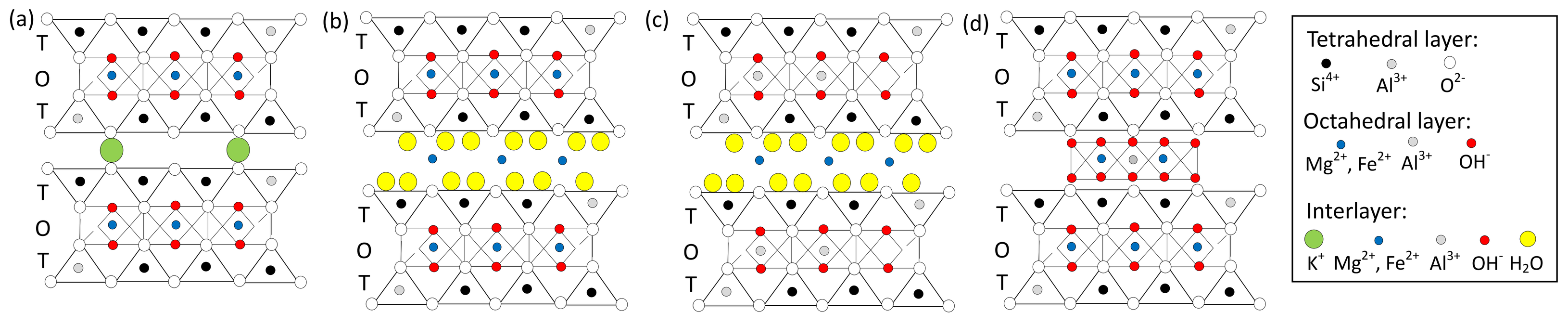

Fig. 4. Representation of ildealized crystal structures of (a) biotite, (b) trioctahedral vermiculite, (c) dioctaherdal vermiculite and (d) chlorite.

EXPERIMENTAL SETUP

- Vermiculitization experiments on biotite have been run in 600 ml Parr reactors at temperatures 50-120°C, under 1 bar partial pressures of CO_2, pH from acid to neutral, and at varying water to rock ratios.
- The starting materials and laboratory products are characterized by SEM-EDX and XRD, as well as by IR spectroscopy to assess spectral consistency of alteration products with remotely-detected phyllosilicates at Oxia.
- Vermiculite has been produced in quasi-open system experiment only i.e., when reactor was open every ~50h, solution extracted and new solution added. In each solution exchange, we made sure to obtain equilibration of solution with CO_2 atmosphere.


Fig. 5. Photograph of Parr reactors used for closed-system vermiculitization experiments.

VERMICULITIZATION OF BIOTITE

- Fe-rich biotite (ferroan phlogopite), grinded and sieved to size of <50 µm has been used in the experiment.
- 1 g of biotite was altered in closed system reactor at pH of 7 and 4 (HCl solutions buffered by 0.1 M NaCl), with water to rock ratio of 20, in temperature of 120°C and under CO_2 dominated atmosphere (1 bar of CO_2). No significant vermiculitization had place, however, under acidic pH, octahedral Fe and tetrahedral Al were partly removed from structure of biotite and deposited as oxides at edges of altered crystals (Fig. 6). Appearance of spectral bands in NIR (Fig.7) may indicate incorporation of interlayer water in experimental product [11, 12]. This suggests fast saturation of solution, due to incongruent dissolution of biotite, that slows down the vermiculitization.
- Quasi-open experiment under acidic pH of 3, with water-rock ratio of 300, in temperature of 65°C led to observable vermiculite formation (Fig. 8). Broadening of peaks in region of biotite 001 and 003 khl diffractions and raise of peak at d=13.9 suggests the newly formed mineral transforms into vermiculite-type structure.

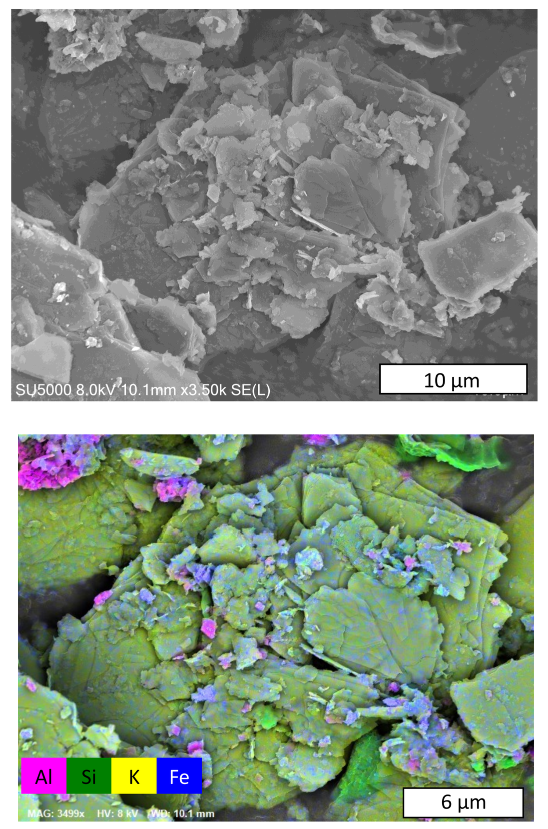

Fig. 6. SEM image and SEM-EDX elemental map composite of experimental product (E-2). Sub-micron-sized Fe-(hydr)oxides and Al-(hydr)oxides are present.

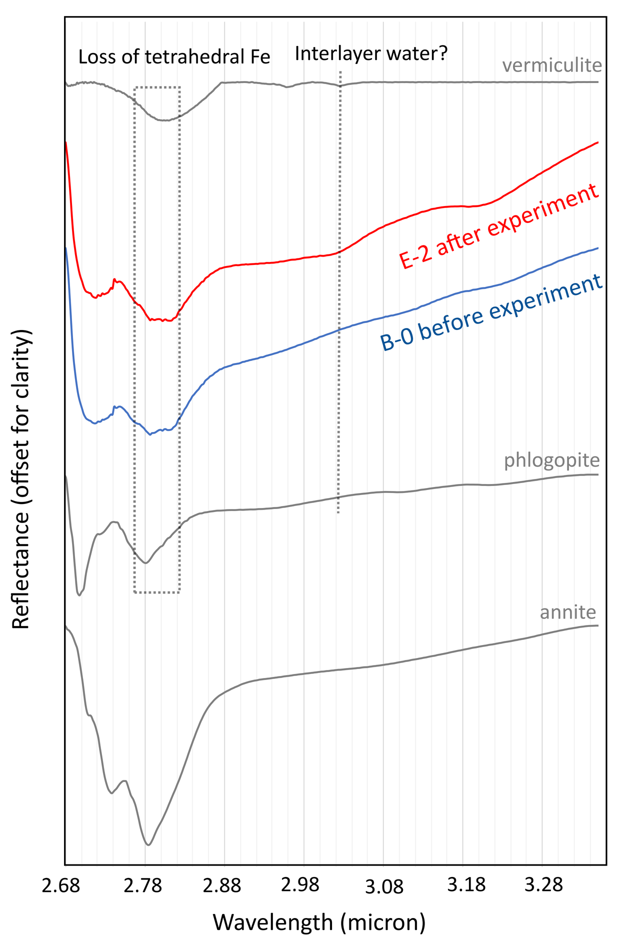

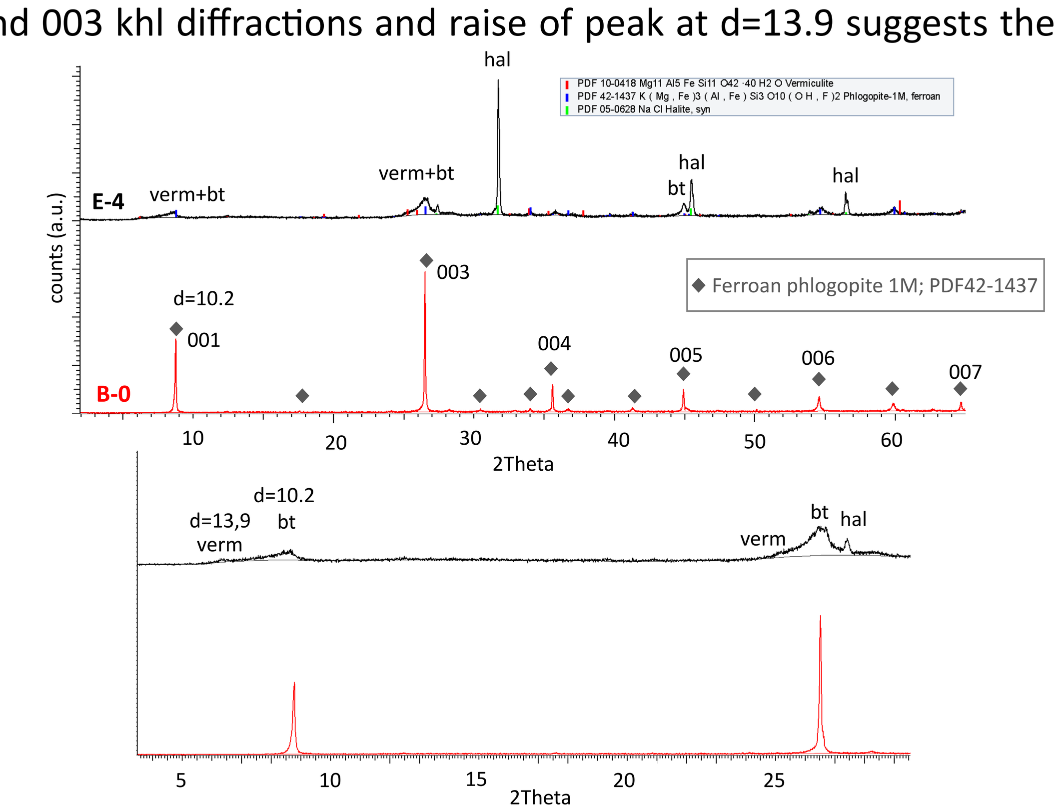

Fig. 8. XRD pattern of starting material (B-0) and products of 25-days of quasi-open experiment under acidic conditions (E-4). The hkl diffractions are indicated above the biotite peaks and charcteristic vermiculite diffractions are shown.

Fig. 7. Continuum-removed NIR spectrum of starting material (B-0) and experimental products in closed system (E-2). For reference, phlogopite (Mg-biotite) and annite (Fe-biotite end-member) spectra are shown as well as vermiculite (LAVE01 RELAB) spectrum is plotted.

Alteration of Fe,Mg-biotite to vermiculite may occur under martian aqueous conditions. Kinetics of reaction for Fe-rich biotite is slow. Alteration requires water delivered in open system.

Acknowledgments: This project has received funding from the European Union's Horizon 2020 (H2020-COMPET-2015) Research and Innovation Program under grant agreement 687302 (PTAL), as well as the Research Council of Norway through its Centres of Excellence funding scheme, project number 223272 (CEED).

References: **[1]** Quantin C. (2016) *LPSC XLVII*, Abstract #2863. **[2]** Carter J. et al. (2016) *LPSC XLVII*, Abstract #2064. **[3]** Carter J. et al. (2015) *Icarus*, 248, 373-382. **[4]** Turner S.M.R. & Bridges J.C. (2017) *LPSC XLVIII*, Abstract #2228. **[5]** Wilson M.J. (2004) *Clay Minerals*, 39, 233–266. **[6]** Bassett W.A. (1961) *X National Conference on Clays and Clay Minerals*, 61–69. **[7]** Banfield J.F. & Murakami T. (1998) *American Mineralogist* 83, 348–357. **[8]** Ross G.J. & Kodama H. (1976) *Clays and Clay Minerals*, 24, 183–190. **[9]** Velasco F. et al. (1981) *Boletín de la Sociedad Española de Mineralogía*, 2, 135–149. **[10]** Sautter V. et al. (2015) Nature Geosciences, 8, 605–609. **[11]** Farmer V.C. et al. (1971) *Mineralogical Magazine* 38: 121–137. **[12]** Swayze G.A. et al., (2018) *American Mineralogist* 103: 517–549. **[13]** Janek M. et al. (2009) Clays and Clay Minerals 57: 416–424.